Influence of the Boreal Autumn Southern Annular Mode on Winter Precipitation over Land in the Northern Hemisphere

TING LIU

State Key Laboratory of Numerical Modeling for Atmospheric Sciences and Geophysical Fluid Dynamics, Institute of Atmospheric Physics, Chinese Academy of Sciences, and University of Chinese Academy of Sciences, Beijing, China

JIANPING LI

College of Global Change and Earth System Sciences, Beijing Normal University, and Joint Center for Global Change Studies, Beijing, China

FEI ZHENG

State Key Laboratory of Numerical Modeling for Atmospheric Sciences and Geophysical Fluid Dynamics, Institute of Atmospheric Physics, Chinese Academy of Sciences, Beijing, China

(Manuscript received 18 October 2014, in final form 5 June 2015)

ABSTRACT

As an atmospheric oscillation with a global scale, the Southern Hemisphere (SH) annular mode (SAM) contributes not only to SH climate variability but also to climate anomalies in the Northern Hemisphere (NH). This paper demonstrates that the strong (weak) boreal autumn SAM usually favors a positive (negative) tripole precipitation pattern in the NH, with more (less) precipitation over the equator and midlatitudes but less (more) precipitation in the subtropics. The corresponding mechanism is examined based on reanalysis data and numerical modeling. It is suggested that the boreal autumn SAM is associated with changes in surface subpolar westerlies, which influence the surface heat exchange and drive the meridional oceanic Ekman flow, redistributing heat near the surface. Through these, warmer (colder) and colder (warmer) sea surface temperature (SST) belts in the SH middle and high latitudes form in response to the positive (negative) boreal autumn SAM, respectively. Such a positive (negative) Southern Ocean SST dipole pattern can persist into the boreal winter via the ''memory'' of SST. It can then affect the vertical motion in the SH meridional circulation and strengthen (weaken) the NH upward and downward branches. These anomalous vertical flows favor a positive (negative) tripole precipitation anomaly pattern in the NH under suitable moisture conditions. Such an ''ocean–atmosphere coupled bridge'' allows the influence of the boreal autumn SAM to persist into the following season and affect the NH climate. Hence, this work suggests that the boreal autumn SAM provides a significant forecasting signal for the NH climate in the following winter.

1. Introduction

The Southern Hemisphere (SH) annular mode (SAM), also known as the Antarctic Oscillation (AAO), is a zonally symmetric ''seesaw'' structure that involves hemisphere-wide fluctuations of air mass between the southern polar region and the midlatitudes (Gong and Wang 1998, 1999; Li and Wang 2003; Li 2005; Limpasuvan and Hartmann 1999; Thompson and Wallace 2000). As the leading mode of atmospheric activity in the SH extratropics, the anomalous SAM can affect the SH sea–air–ice system and other climate variables through variations in the strength of the circumpolar winds in middle and high latitudes that induce anomalous surface heat exchange. Zonal wind anomalies also affect the oceanic meridional Ekman transport, which is associated with redistribution of heat near the surface. These processes can imprint the SAM signature

Denotes Open Access content.

Corresponding author address: Dr. Jianping Li, Dean and Professor, College of Global Change and Earth System Sciences, Beijing Normal University, Beijing 100875, China.
E-mail: ljp@bnu.edu.cn

DOI: 10.1175/JCLI-D-14-00704.1

onto sea surface temperature (SST; Carleton 2003; Hall and Visbeck 2002; Sen Gupta and England 2006). Thus, the SAM has a major influence via air–sea interaction on the regional climate (Fogt et al. 2012; Gillett et al. 2006; Thompson and Solomon 2002) in, for example, Antarctica (Marshall et al. 2006), South America (Silvestri and Vera 2003), Australia (Feng et al. 2010; Hendon et al. 2007), New Zealand (Kidston et al. 2009; Renwick and Thompson 2006; Ummenhofer and England 2007; Ummenhofer et al. 2009), and South Africa (Reason and Rouault 2005). Meanwhile, the variability and distribution of sea ice around Antarctica are also regulated by the SAM through a combination of atmospheric, oceanic dynamic, and thermodynamic forcing as well as by an albedo feedback mechanism that allows ice extent anomalies to persist for many months (Hall and Visbeck 2002; Lefebvre et al. 2004; Liu et al. 2004; Sen Gupta and England 2006; Yuan and Li 2008).

The SAM contributes not only to climate change in the SH but also to climate anomalies in the Northern Hemisphere (NH; Zheng et al. 2014; Zheng et al. 2015; Li 2016). In recent years, the influence of the SAM on NH climate anomalies has received considerable attention. Initial interest focused on the effect of the boreal spring SAM on East Asia. There is a significant negative correlation between the boreal spring SAM and the following East Asian summer monsoon (EASM; Nan and Li 2003, 2005a,b), in which the ''ocean–atmosphere coupled bridge'' (Li et al. 2013; Li 2016) plays an important role. The boreal spring SAM is also significantly negatively correlated with dust weather frequency in northern China (Fan and Wang 2004). The boreal winter SAM also influences the summer climate of East Asia. Wu et al. (2006a,b) reported that the preceding boreal winter SAM was associated with what they termed drought–flood coexistence and drought–flood abrupt alternation in the middle and lower reaches of the Yangtze River in the following summer. For the boreal winter climate, Wu et al. (2009) pointed out that the boreal autumn SAM also affected decadal variability of the Chinese winter monsoon. The November–December SAM can also modulate the variability of the Intertropical Convergence Zone (ITCZ) in the Pacific by the related dipole SST anomalies (SSTAs) in the South Atlantic–Pacific. Subsequently, a distinguished atmospheric teleconnection pattern is induced and prevails over the NH midlatitude region as a response to the anomalous ITCZ. And winter precipitation over East Asia responds to this cross-equatorial propagation of the SAM signal (Wu et al. 2015). Boreal spring precipitation is also affected. Zheng and Li (2012) found that positive (negative) SAM events in the preceding boreal winter could lead to less (more) spring precipitation in southern China. The boreal spring SAM also had a significant effect in other regions—for example, on the North American summer monsoon (Sun 2010) and West African summer monsoon (Sun et al. 2010).

We note that the ocean–atmosphere coupled bridge has been referred to as a key process by which the SAM influences the NH climate (Nan and Li 2003, 2005a,b; Wu et al. 2009; Zheng and Li 2012). The SAM signal can be imprinted onto SST through air–sea interaction. The ''memory'' characteristic of SST means that the anomalous signal can persist or be transmitted over a long period and impacts the regional climate in the following season via air–sea interaction (Li 2016). In general, previous research (Ciasto and Thompson 2008; Zheng and Li 2012) indicated that the abnormal SAM events favored belts of SSTAs that were out of phase between the SH middle and high latitudes. The positive (negative) SAM events were usually associated with cold (warm) SST poleward of 45°S and warm (cold) SST equatorward of 45°S. The anomalous heating caused by these SAM-related SSTAs induced adjustment of the meridional circulation, which had an important effect on the regional climate anomalies. Sen Gupta and England (2006) showed that there were remarkable correlations between SAM anomalies and cloud cover, water vapor, and precipitation, characterized by a zonally symmetric seesaw pattern between the subtropical and mid–high latitudes in the SH. Boer et al. (2001) also suggested that the SAM influenced water vapor balance in the SH through the meridional circulation and caused the out-of-phase precipitation anomalies in the SH subtropical and mid–high latitudes. The two hemispheres share a branch of the meridional circulation, so do the SAM changes have a significant zonally symmetric impact on precipitation in the NH? Can the preceding season's SAM provide a forecasting signal for the NH winter precipitation? These questions deserve our attention. Moreover, winter snowstorms have frequently occurred in the NH in recent years and caused huge economic losses, such as the peculiar snowstorm in southern China in 2008 and the cold and snowy weather experienced in Europe and North America during 2013. Thus, it is timely to search for a new predictor that may improve the forecast skill for the NH winter climate.

In this context, we will focus on the relationship between the boreal autumn SAM and the winter precipitation anomalies in the NH, mainly from a zonally averaged perspective, and examine possible mechanisms. The paper is organized as follows. In section 2, we provide a brief review of the data and methods used in the analysis. Section 3 describes the relationship between the boreal autumn SAM and precipitation anomalies in the following winter. The NH circulation anomalies related to the anomalous boreal autumn SAM are also presented in this section. On the basis of these results,

possible physical mechanisms are discussed in section 4. In the final section, the main conclusions are summarized and some outstanding issues are presented.

2. Data and methodology

a. Data

We used the following main datasets: 1) Land precipitation data were obtained from the Global Precipitation Climatology Centre (GPCC) dataset (Rudolf and Schneider 2005), with a horizontal resolution of 0.5° × 0.5°; 2) atmospheric variables, such as sea level pressure (SLP), winds, vertical velocity, and relative humidity, were extracted from the European Centre for Medium-Range Weather Forecasts (ECMWF) interim reanalysis (ERA-Interim) globally archived dataset (Dee et al. 2011), with a horizontal resolution of 2.5° × 2.5°; 3) the SST data were taken from the Extended Reconstructed SST version 3 (ERSST v3; Smith et al. 2008), with a horizontal resolution of 2° × 2°; and 4) the ENSO index (Niño-3.4) was taken from the NOAA Climate Prediction Center's website (http://www.cpc.ncep.noaa.gov/data/indices/). We also employed another land precipitation dataset [the NOAA Precipitation Reconstruction over Land (PREC/L; Chen et al. 2002)] and two global precipitation datasets [the Global Precipitation Climatology Project (GPCP; Adler et al. 2008; Huffman and Bolvin 2011) v2.2 and the Climate Prediction Center (CPC) Merged Analysis of Precipitation (CMAP; Xie and Arkin 1997)] to validate the results for precipitation. There were no major biases of different products, especially over land. As the available precipitation products demonstrate superior statistics over land where gauge data have been incorporated (Adler et al. 2001), we used the land precipitation data in this research.

In respect of atmospheric circulation, similar results could be derived by applying the same technique to the National Centers for Environmental Prediction–National Center for Atmospheric Research (NCEP–NCAR) reanalysis (Kalnay et al. 1996), which gave us confidence to endorse the conclusion here. Meanwhile, considering the reliability of data in the SH, we focused our analysis on monthly data for the more recent period of 1979–2010, for which satellite records were available. The boreal season in this article includes autumn and winter, which are defined as September–November (SON) and December–February (DJF), respectively.

b. Methodology

The SAM index (SAMI) in this article is defined as the difference in the normalized monthly zonal-mean SLP between 40° and 70°S (Nan and Li 2003; http://ljp.gcess.cn/dct/page/65609), which is a modification of the AAO index defined by Gong and Wang (1999).

We used a variety of statistical methods to investigate the influence of the boreal autumn SAM on winter precipitation, including singular value decomposition (SVD), simultaneous and lead–lag correlation, and composite analysis. High- and low-SAMI cases were identified as the fluctuations of the index beyond one standard deviation. Composite difference refers to the difference in the corresponding elements between the high- and low-SAMI cases. To eliminate the influence of the ENSO signal in our calculations, and thus highlight the role of the SAM, we used partial correlation analysis.

The significance of the correlation between two autocorrelated time series, such as SST in this work, was accessed using the effective number of degrees of freedom n^{eff}, which could be given by the following approximation (Li et al. 2012; Pyper and Peterman 1998):

$$\frac{1}{n^{\text{eff}}} = \frac{1}{n} + \frac{2}{n}\sum_{j=1}^{n}\frac{n-j}{n}\rho_{XX}\rho_{YY}, \tag{1}$$

where n is the sample size, and $\rho_{XX}(j)$ and $\rho_{YY}(j)$ are the autocorrelations of two sampled time series X and Y, respectively, at time lag j.

It is well established that eddies sustain the anomalous flow associated with annular mode excursions (Limpasuvan and Hartmann 2000; Lorenz and Hartmann 2001). Under quasigeostrophic scaling, the zonal-mean thermodynamic energy equation (Holton and Hakim 2012, 318–319; Zheng et al. 2015) on the midlatitude β plane is

$$\frac{\partial[T]}{\partial t} = -\frac{\partial[T^*v^*]}{\partial y} - \frac{N^2H}{R}[w]. \tag{2}$$

The variable v is meridional wind, w is vertical velocity, T is air temperature, N is the Brunt–Väisälä frequency, H is the atmospheric scale height, and R is the gas constant. Square brackets indicate the zonal mean, the asterisk denotes the zonal deviation, and other symbols carry their usual meaning. For steady-state mean flow conditions, the tendency terms of Eq. (2) can be neglected so that the adiabatic cooling/heating is balanced by the convergence/divergence of the eddy heat flux; which means convergence of the eddy heat flux favors upward movement while divergence comes with downward movement (Holton and Hakim 2012; Zheng et al. 2015). We employed the above dynamic equation in a diagnostic analysis of the possible physical mechanism by which the boreal winter meridional circulation responds to the autumn SAM.

To gain more insight into the influence of the boreal autumn SAM on precipitation in the following NH

winter, we carried out numerical experiments using the NCAR Community Atmospheric Model version 5 (CAM5). The horizontal resolution used was T42 (approximately 2.8° × 2.8°), with 26 hybrid vertical levels. (A complete description of this model version is available online at http://www.cesm.ucar.edu/models/cesm1.0/cam/docs/description/cam5_desc.pdf.)

3. Boreal winter precipitation over land in the NH associated with the previous autumn SAM

a. *Linkage between the boreal autumn SAM and winter precipitation*

Figure 1a presents the correlation coefficients between the boreal autumn SAMI and precipitation in the following NH winter over land. There is a significant zonally symmetric positive tripole (+, −, +) pattern in the meridional direction. The positive values cover the equator and midlatitude regions, with negative values over the subtropics. The regions where the correlation coefficients are significant at greater than a 90% confidence level (the stippled areas) also show the positive tripole distribution. These features imply that a strong (weak) boreal autumn SAM is likely to be followed by increased (reduced) winter precipitation over the equator and midlatitude regions but reduced (increased) precipitation over the subtropics. In addition, as there are many factors that affect local precipitation, the variance contribution varies from each other, and thus it is reasonable that some zonal asymmetry exists in the correlation maps between the boreal autumn SAM and winter precipitation. This may require further research into the local traits of the climate, but that is beyond the scope of the present study. In this work, we focus only on the zonal symmetric feature of the boreal winter precipitation affected by the autumn SAM.

There is ample evidence to suggest that ENSO plays an important role in the climate anomalies that develop in the NH. At the same time, there are mutual influences between ENSO and the SAM (Ding et al. 2012, 2015; Fogt and Bromwich 2006; Liu et al. 2002; L'Heureux and Thompson 2006; Sen Gupta and England 2006). Therefore, we must consider whether the results above are the consequence of ENSO or independent of it. To resolve this issue, we used partial correlation analysis (Fig. 1b). Comparing Fig. 1b with Fig. 1a shows that the distribution of the correlation coefficients is mostly unchanged after excluding the ENSO signal. There is a slight decrease in the size of the regions that are significant at a confidence level greater than 90%. This could be due to the greater contribution of ENSO compared with the SAM over these particular areas. Further research is needed. Even so, based on the partial correlation analysis mentioned above, it indicates that the relationship between the boreal autumn SAM and winter precipitation in the NH still exists without the influence of ENSO. Thus, the boreal autumn SAM is one possible factor that can affect winter precipitation in the NH.

Figure 1c shows the correlation coefficients between the boreal autumn SAMI and the global zonal-mean winter precipitation in the NH (the solid red line), and the tripole pattern is more obvious. There are regions of significant (>90%) correlation over the equator (1°–14°N), in the subtropics (24°–37°N), and in midlatitude regions (44°–58°N). We then represent the winter precipitation using regional precipitation indices that are defined as the standardized regional average winter precipitation for the above three regions. There are significant relationships between the SAMI and the three regional precipitation indices at a confidence level greater than 95%, with correlation coefficients of 0.49, −0.53, and 0.43, respectively. This further proves that the strong (weak) boreal autumn SAM is often followed by more (less) winter precipitation over the equator and midlatitude regions but less (more) precipitation in the subtropics. The solid blue line is the result after the removal of the ENSO signal and linear trend. The tripole pattern of precipitation anomalies is not severely impacted by the ENSO and linear trend, except for some decrease in the significance areas. This confirms the reliability of the relationship between the boreal autumn SAM and winter precipitation.

To further isolate the coupled relationship between the boreal autumn SAM and winter precipitation in the NH, SVD was applied to the boreal autumn SLP anomalies in the extratropical SH over the domain poleward of 20°S and the following winter's precipitation anomalies in the NH. The leading mode (Fig. 2) accounts for 36% of the total covariance. The two time series are significantly correlated (>99% confidence level), with a coefficient of 0.83. The atmospheric signal is characterized by the feature of the positive phase of the SAM with an out-of-phase SLP pattern between high and midlatitudes in the SH. The boreal winter precipitation field in the NH has a zonal belt feature with a positive tripole pattern. When the boreal autumn SAM is in its strong positive phase, positive winter precipitation anomalies occur over the equator and midlatitude regions but negative anomalies occur over the subtropics. This further supports the hypothesis that the boreal autumn SAM may influence precipitation in the following NH winter.

b. *Connections between the boreal autumn SAM and winter atmospheric circulation anomalies*

Precipitation anomalies are affected by the combined influence of water vapor conditions and vertical motion. In this paper, composite analysis was used to explore the

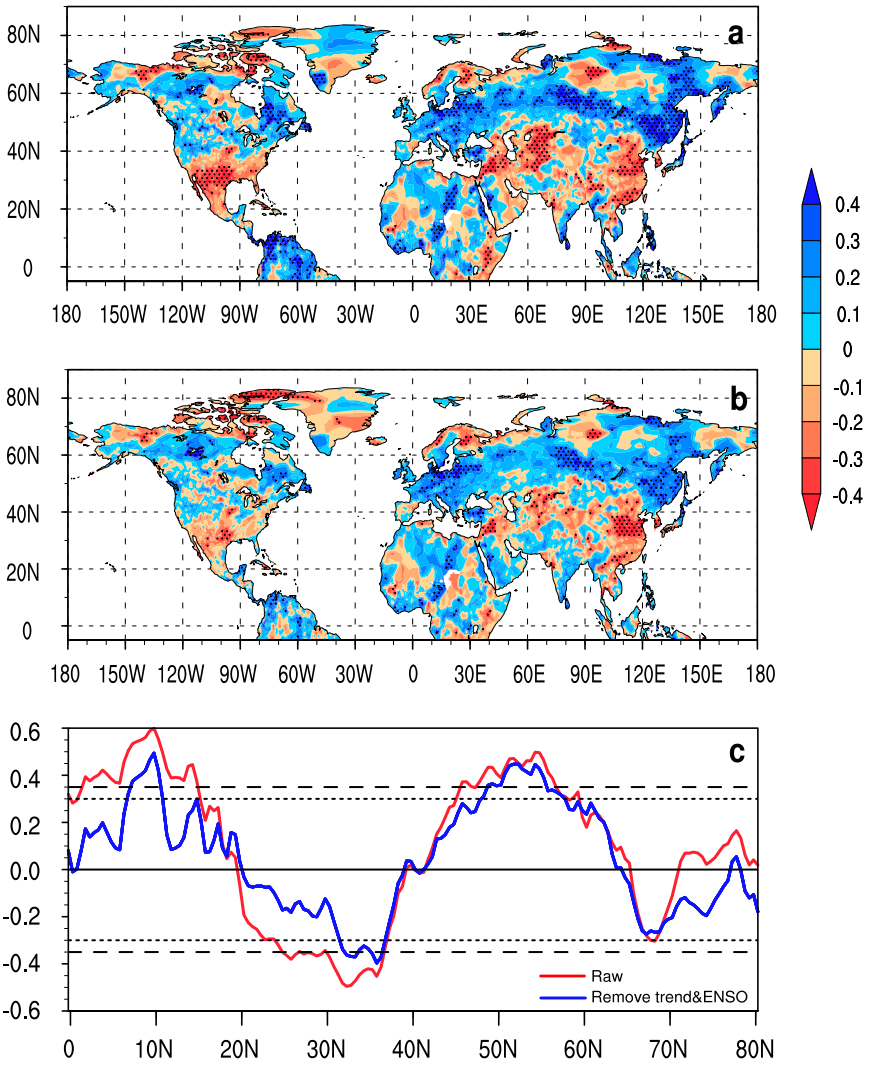

FIG. 1. Correlation coefficients between the boreal autumn SAMI and winter precipitation over NH land. (a) Correlation map before removal of trend and ENSO. (b) Partial correlation after removal of trend and ENSO. (c) Correlation map of zonal-mean precipitation (red line) and partial correlation after removal of trend and ENSO (blue line). The stippled areas in (a) and (b) indicate significance at the 90% confidence level using Student's *t* test. In (c), the short and long dashed lines indicate significance at the 90% and 95% confidence levels, respectively.

boreal winter circulation anomalies associated with the preceding autumn SAM.

Figure 3 displays the height–latitude section of the composite differences of zonal-mean meteorological variable anomalies for the boreal winter between the high and low boreal autumn SAMI. When the boreal autumn SAM is strong (weak), the Ferrel cell is strengthened (weakened) south of 40°S, which is coincident with previous studies (Zheng and Li 2012). Meanwhile, anomalous ascending (descending) motion (Fig. 3a) appears centered over 10° and 55°N, and there is anomalous descending (ascending) motion near 30°N (Fig. 3a). In addition, the configuration of the divergence field in the upper- and lower-tropospheric layers (not shown) matches these vertical motion anomalies well.

The composite differences in meridional circulation also show that in the high (low) boreal autumn SAMI years, the anomalous upward and downward motion (vectors) superimposed on the climatic mean states (shading) strengthens (weakens) the upward branches near the equator and midlatitude regions and the downward branch over the subtropics (Fig. 3c) in the NH.

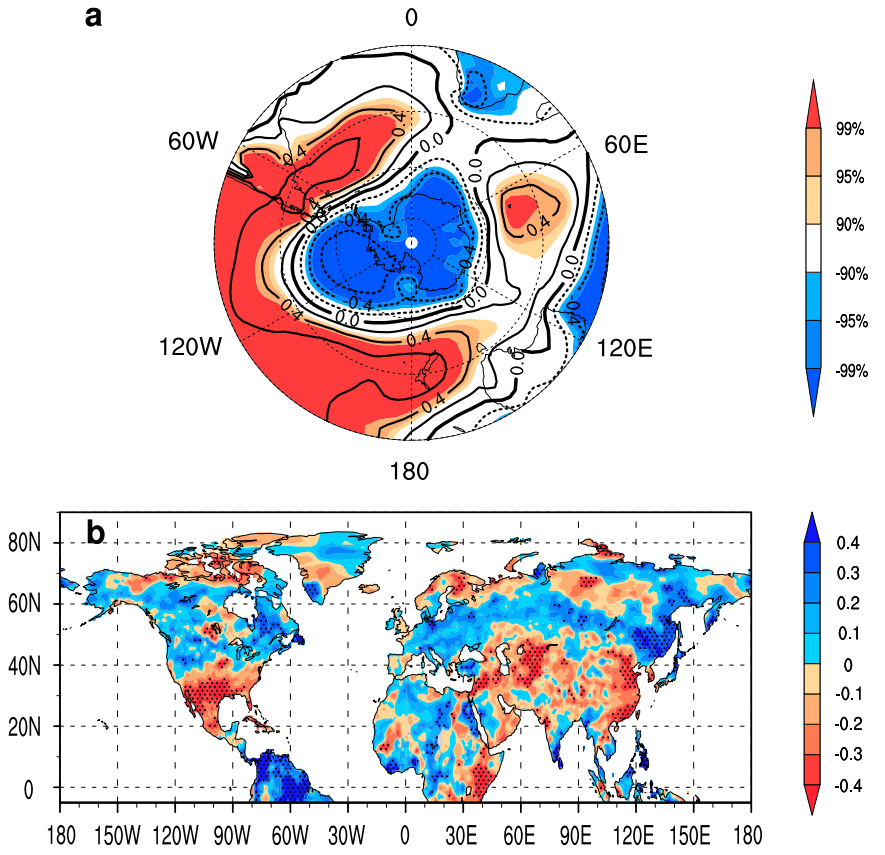

FIG. 2. Heterogeneous correlation patterns of the leading SVD mode for (a) the boreal autumn SH SLP anomalies south of 20°S and (b) the boreal winter precipitation anomalies in the NH. The shaded and stippled areas in (a) and (b) indicate significance at and over the 90% confidence level using Student's *t* test. The latitude lines in (a) are at 20° intervals starting from 20°S.

Figure 3b presents the composite differences for relative humidity. For the high (low) boreal autumn SAMI cases, positive (negative) anomalies appear at about 10° and 55°N, and negative (positive) anomalies at about 30°N in the middle and lower troposphere, indicating that the air is wetter (drier) near the equator and midlatitude regions and drier (wetter) over the subtropics. Note that there are differences in the changes of relative humidity at midlatitudes between ERA-Interim and NCEP data. There are significantly positive anomalies at 50°–60°N in the NCEP data (not shown), but the positive anomalies are relatively small in the ERA-Interim data. Even so, the vapor conditions associated with the boreal autumn SAM have the potential to match the vertical motion necessary to favor the tripole pattern of the winter precipitation.

In brief, in the case of the positive boreal autumn SAM, the anomalous horizontal convergence at low levels and divergence at high levels are associated with a strong boreal autumn SAM that favors upward motion of wetter air in the equatorial and midlatitude regions but favors the opposite over the subtropics. The combination of the divergence field, vertical motion, and suitable water vapor conditions favors the occurrence of the positive tripole pattern of winter precipitation anomalies in the NH. When the boreal autumn SAM is in the opposite phase, the pattern reverses.

4. Possible physical mechanisms

As noted above, the boreal autumn SAM is associated with NH precipitation anomalies in the following winter. Accordingly, we now investigate the physical processes that might be responsible for this relationship. Given the relatively weaker persistence of the atmosphere, we will take the ocean–atmosphere coupled bridge (Li et al. 2013; Li 2016) into consideration.

a. SST associated with the boreal autumn SAM

Figure 4 presents the lead–lag correlation between surface zonal wind speed and the boreal autumn SAMI. There is a significant dipole pattern that persists from

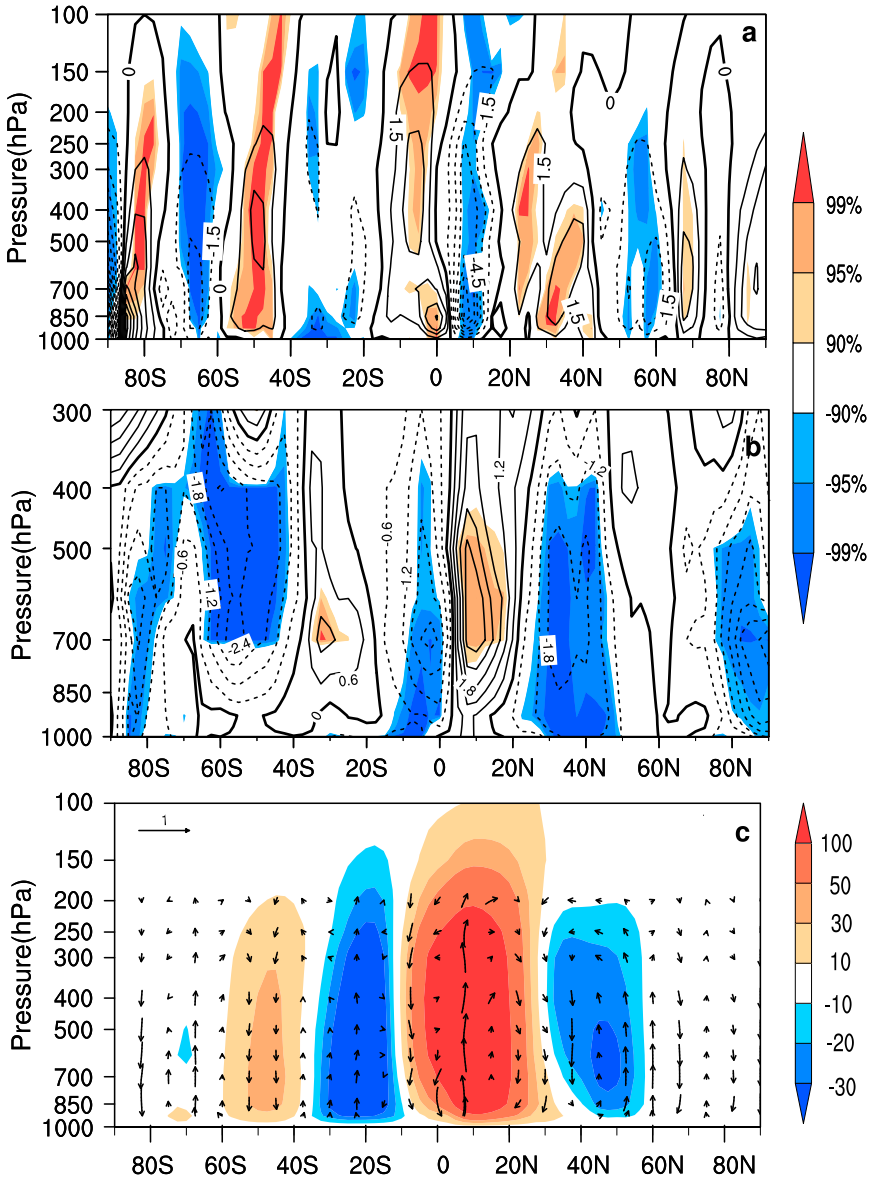

FIG. 3. Composite differences between high and low boreal autumn SAMI years of zonal-mean boreal winter (a) vertical velocity (10^{-5} Pa s^{-1}), (b) relative humidity (%), and (c) meridional circulation (vectors). Contours in (a) and (b) show the composite differences, and the anomalies that are significant at the 90% confidence level are shaded. In (c), the shading indicates the climatological mean boreal winter mass stream function (10^9 kg s^{-1}).

the boreal autumn to winter in SH middle and high latitudes. During the strong boreal autumn SAM cases, positive correlations occur over 45°–70°S, and negative correlations are centered on 30°S. Because of the prevailing westerlies south of 30°S, the westerly winds weaken over 30°S and strengthen within 45°–70°S. The situation for a weak SAM is the opposite. The zonal wind anomalies can persist from boreal autumn through winter. This might be related to wave–mean flow interaction, which has the potential to influence the strength and persistence of the SAM. Specifically, an anomalous SAM can alter local baroclinicity and storminess by affecting temperature gradients, as discussed next. The increase in storms means greater momentum flux into the upper troposphere as these eddies decay, increasing the near-surface westerlies (a more positive SAM), and vice versa (Chen et al. 2010; Frierson et al. 2007; Hartmann and Lo 1998; Limpasuvan and Hartmann 1999, 2000; Lorenz and Hartmann 2001; Marshall and Connolley 2006).

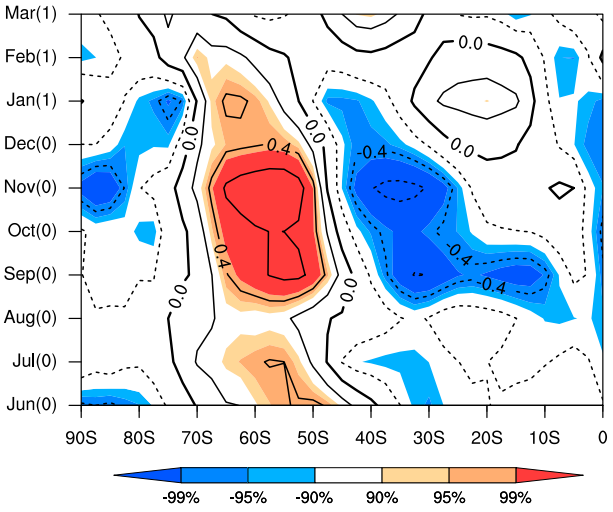

FIG. 4. Lead–lag correlation coefficients between the boreal autumn SAMI and zonal-mean 10-m zonal wind from June (0) to the next March (1). The simultaneous year is denoted by 0, and 1 denotes the following year. The shaded areas indicate significance at and over the 90% confidence levels using Student's *t* test.

Surface zonal wind anomalies play an important role in latent and sensible heat exchange at the air–sea interface and also induce surface meridional oceanic Ekman transport associated with the advection of heat. These two processes can further affect the SSTAs (Sen Gupta and England 2006). Our results indicate that a positive boreal autumn SAM is usually associated with strong surface westerlies south of 45°S and weak surface westerlies over the region 30°–45°S. High wind speed contributes to increases in ocean heat release and equatorward Ekman transport of cold water, leading to negative SSTAs at high latitudes, whereas a weaker westerly wind gives the opposite in midlatitudes. When the boreal autumn SAM is in its negative phase, the situation is reversed. This is seen clearly in the composite differences of boreal autumn SSTAs between the high and low autumn SAMI cases (Fig. 5a). In the boreal autumn positive (negative) SAM case, SST is warmer (colder) over 30°–45°S and colder (warmer) over 45°–70°S, and this pattern can persist to winter (Fig. 5b).

For convenience, this SAM-related dipole-like SSTA is referred to as the Southern Ocean dipole (SOD; Li 2016), which mainly reflects out-of-phase latitude band variations in SSTAs between the high and midlatitudes in the SH. We employ two approaches to define the SOD index (SODI). One is defined as the difference of the normalized monthly zonal-mean SST between 40° and 60°S, which is the latitude of the maximum negative cross-correlation of SST. The other is formed by projecting monthly mean Southern Ocean SSTAs onto maps of Southern Ocean SSTAs regressed onto standardized values of the boreal autumn SAM, which follows the work of Ciasto et al. (2011). The two SODIs are highly correlated, with correlation coefficients of 0.86 and 0.89 in boreal autumn and winter, respectively. Both can reflect the variability of the meridional SST gradient, which is the principal characteristic associated with SOD. As these two methods are in close agreement with each other, we present only the result based on the former SODI.

b. *Response of the meridional circulation to SOD in the boreal winter*

Diagnostic analysis shows that the anomalous boreal autumn SAM is often followed by a SOD pattern during boreal autumn and winter, as the correlation coefficients between the boreal autumn SAMI and the SODI in autumn and winter are 0.72 and 0.63, respectively, which are significant at the 99% confidence level using the effective numbers of degrees of freedom. This is consistent with a previous study by Zheng and Li (2012) showing that leading SAM anomalies favor the dipole SST anomaly pattern. Zheng and Li (2012) attributed this phenomenon to the large heat capacity of the ocean, with a lagged autocorrelation of the boreal autumn SODI of 0.81, which is significant at the 99% confidence level using the effective numbers of degrees of freedom. This suggests that the preceding anomalous SAM signal can be stored in the ocean by affecting the surface heat flux exchange and the oceanic Ekman transport, and this anomalous SST can persist to the next season to impact the atmospheric circulation and regional climate via air–sea interaction, which is exactly the embodiment of ocean–atmosphere coupled bridge (Li 2016). Thus, can the boreal autumn SAM affect the following winter precipitation in the NH through the SOD, and if so, by what mechanism?

We investigated the composite differences between SODI and the zonal-mean vertical velocities in the boreal winter (Fig. 6). When the boreal winter SOD is in its positive phase, there is significant downward motion centered over 50°S (shading), indicating a strengthening of the Ferrel cell south of 40°S. Meanwhile, significant upward motion occurs at around 30°S (shading). The anomalous vertical movement induces an adjustment of the meridional circulation in the SH. As the global meridional circulation in the two hemispheres shares the same upward branch, adjustments of the SH meridional circulation also affect the NH meridional circulation, with anomalous upward motion centered at 10° and 50°N and anomalous downward motion at 20°–30°N. This situation is reversed for a negative boreal winter SOD case. It is also consistent with the results of the diagnostic analysis in section 3 and suggests that the SOD plays a bridging role between the boreal autumn SAM and the following winter's precipitation in the NH.

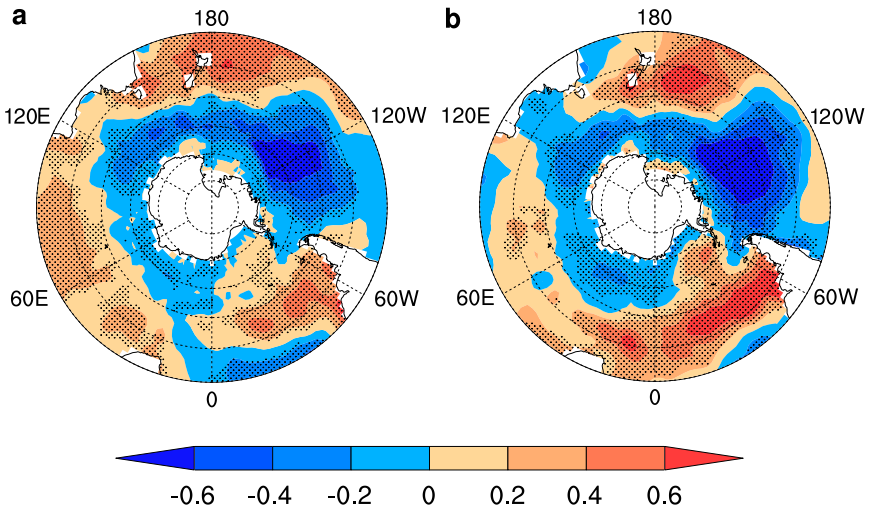

FIG. 5. Composite differences of boreal (a) autumn SST and (b) winter SST (°C) between high and low autumn SAMI cases. The stippled areas indicate significance at the 90% confidence level using Student's *t* test. The latitude lines are at 10° intervals starting from 30°S.

c. *Mechanism of meridional circulation responses to the SOD in the boreal winter*

As presented in Fig. 5, the SOD presents a seesaw characteristic in the meridional direction, which means the anomaly meridional gradient of extratropical SST. Prior work suggests that this meridional SST gradient plays an effective role in modulating the local baroclinicity, which favors the activities of eddies and involves modifications to the convergence and divergence of the eddy heat flux. Subsequently, corresponding adjustments of vertical movement are induced, as well as a meridional circulation response to the meridional SST gradient through wave–mean flow interaction (Chen et al. 2010; Frierson et al. 2007; Hartmann and Lo 1998; Hoskins and Karoly 1981; Limpasuvan and Hartmann 2000; Marshall and Connolley 2006).

Figure 7a displays the correlation coefficients between the SODI and the meridional gradient of SH extratropical SST in the boreal winter. It is seen that the SST

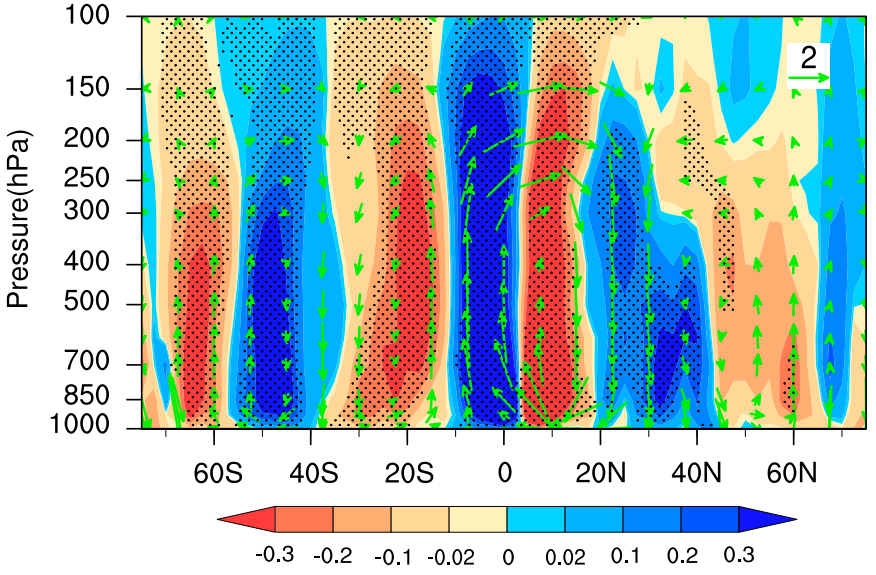

FIG. 6. Composite differences of the boreal winter vertical velocity (10^{-4} Pa s^{-1}) based on the boreal winter SODI (shading). The red (blue) shading corresponds to upward (downward) motion. The vectors represent the climatological-mean boreal winter meridional circulation. The stippled areas indicate significance at the 90% confidence level using Student's *t* test.

gradient is significantly increased between 42° and 57°S but decreased south of 57°S. These SST gradient anomalies directly affect the local baroclinicity, which manifests as the enhanced gradient of potential temperature south of 50°S but reduced north of 50°S (not shown). As discussed above, the changes of local baroclinicity have a profound impact on the activities of eddies and involves modifications to the convergence and divergence as shown in Fig. 7b. In the case of the positive (negative) boreal winter SOD, the anomaly divergence occurs in the lower troposphere and convergence occurs in the upper troposphere centered on 50°S. But the situation is reversed near 30°S. This configuration of the divergence field matches the anomalous descent and ascent in the troposphere at around 50° and 30°S.

The activities of eddies induced by the anomalous local baroclinicity are accompanied by the convergence/divergence of eddy heat flux, which can balance the adiabatic cooling/heating. Figure 7c presents the correlation coefficients between the convergence of the eddy heat flux and the SODI in the boreal winter. During the positive boreal winter SOD, anomalous divergence and convergence of eddy heat flux center on 50° and 30°S, respectively, which interprets the anomalous upward and downward motion near 30° and 50°S (Fig. 6). The situation is opposite in the negative boreal winter SOD cases. In addition, note that the association between meridional circulation variations and the SOD extends as far as the NH. The anomalous activities of eddies and the related wave–mean flow interactions in terms of changes in convergence/divergence of eddy heat flux are also in accordance with the descent and ascent anomalies near 10°–20°, 30°, and 50°N.

In general, the possible mechanisms for explaining the influences of the boreal autumn SAM on the winter meridional circulation and precipitation are proposed based on air–sea interactions and wave–mean flow interactions. The anomalous boreal autumn SAM signal can be sustained by SOD and persists to the following winter. This changes the meridional SST gradient and local baroclinicity, which induce the anomalous eddy activities. The related convergence/divergence of the eddy heat flux balances the diabatic cooling/heating by adjustments of the vertical movement. And the meridional circulation exhibits corresponding adjustments to the SAM-related SOD. Specifically, the strong (weak) boreal autumn SAM is followed by a strengthening (weakening) of the NH meridional circulation.

d. Numerical experiments in CAM5

To further verify that the above physical mechanisms explain the winter SOD impact on the global meridional circulation, numerical experiments were conducted using the CAM5 model described in section 2. The control run was driven by climatological SST. To isolate and mimic the impacts of the boreal winter SOD on the winter circulation, we designed two pairs of the experiments. In the first pair (EA), the only difference between the control and positive (negative) sensitivity experiments was that a constant SSTA based on the composition pattern of SSTAs onto the positive (negative) winter SODI was imposed onto the winter SH extratropics SST climatology. In the second pair (EB; the idealized experiments), SH extratropical ocean SSTs are increased and decreased; the changes describe a sine wave centered on 50°S with a wavelength of 40° latitude so that values at 30° and 70°S are unchanged and with an amplitude of 1°C on 60° and 40°S. All experiments were integrated for 30 years, and outputs from the last 20 years were used for the analysis to reduce the uncertainties in model spinup caused by initial conditions.

Figure 8 presents the composite differences of the meridional circulation between the positive and negative boreal winter SOD experiments in each pair. The response of the vertical velocity to the SOD is generally consistent in the two pairs of experiments and also in line with the observations. The positive SOD anomalies usually excite ascending anomalies over 30°–40°S and descending anomalies centered on 50°S (shading), which induce an adjustment of the meridional circulation. As the meridional circulation in the two hemispheres shares the same upward branch, the NH meridional circulation also responds to the positive SOD anomalies with anomalous upward motion centered on 10° and 50°N (north of 55°N in the EB; Fig. 8b) and anomalous downward motion at around 30°N, as well as the strengthening of the upward and downward branches (vectors in Fig. 8) in the NH. When the SOD is in a negative phase, this situation is reversed. These kinds of vertical motion anomalies can affect the precipitation anomalies in the NH under suitable water vapor conditions.

In addition, it should be noted that the response of the vertical motion to the SOD is slightly weaker in the observations, especially in the NH. And as the SSTA pattern in the EA is based on the observed SST, the response in EA (Fig. 8a) is probably nearer reality compared with the EB (Fig. 8b), in which the structure is relatively fragmentary in the NH and the anomalous ascent in the midlatitudes is farther north than that in the observations. As there is a positive feedback mechanism between the SOD and SAM (e.g., Hartmann and Lo 1998; Limpasuvan and Hartmann 1999, 2000; Lorenz and Hartmann 2001; Marshall and Connolley 2006), in which the SOD has an effect on the SAM and meridional circulation via wave–mean interaction and the

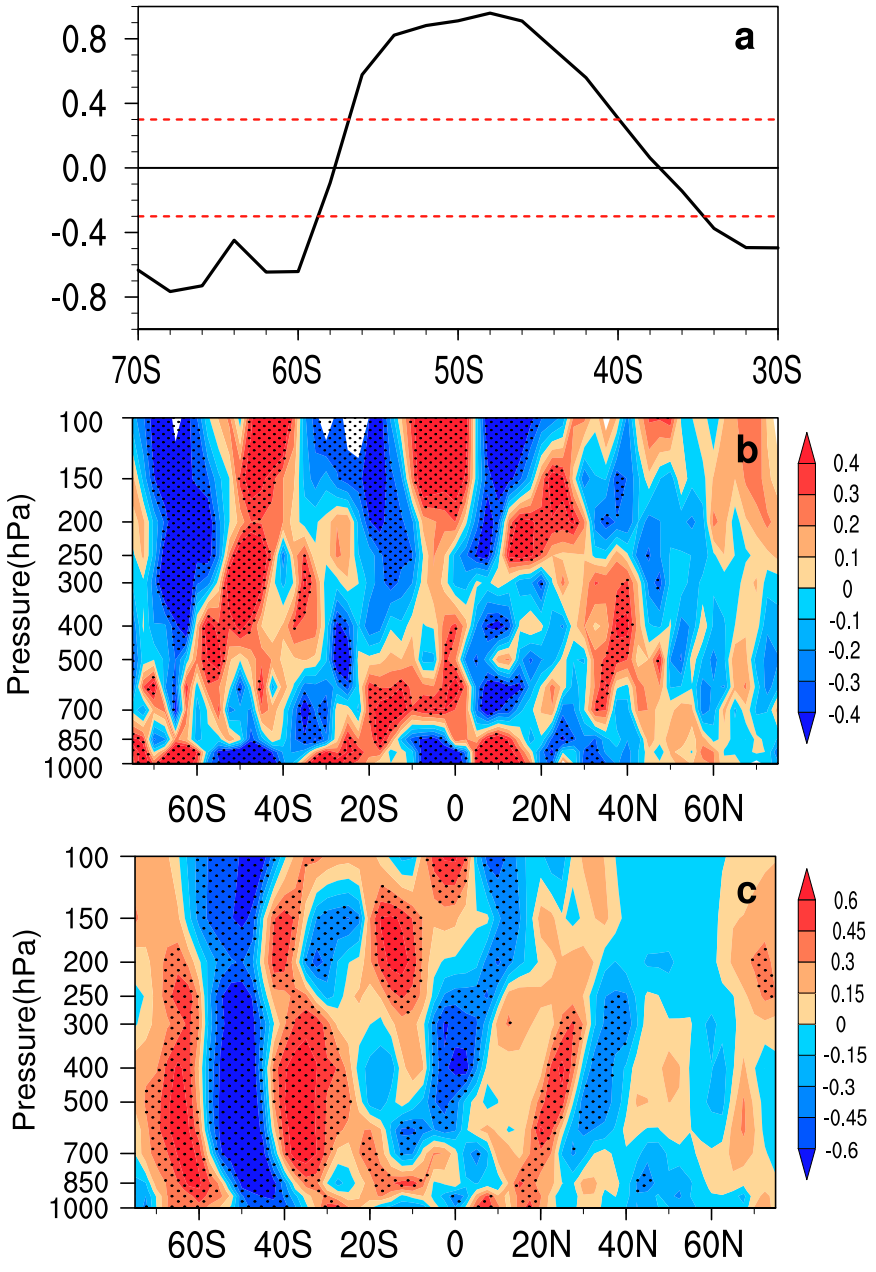

FIG. 7. Correlation coefficients between the boreal winter SODI and (a) winter meridional gradient of zonal-mean SST, (b) winter convergence, and (c) winter convergence of eddy heat flux. The stippled areas indicate significance at the 90% confidence level using Student's *t* test.

SAM influences the SOD by dynamic and thermodynamic processes, the observed composites reflected the coupled effects of the SAM and SOD on meridional circulation. Given the AGCM simulation without air–sea interactions, the meridional circulation response is reflective of the anomalies associated with the initial SOD other than in the observations. Thus, the aforementioned differences between the simulation and observations are inevitable. Nevertheless, the experiments approximately capture the major characteristics of the observations mentioned above (Fig. 6). This confirms the hypothesis that SOD acts as a bridge to implement the impact of boreal autumn SAM on winter circulation.

5. Discussion and conclusions

In this work, we focused on the relationship between the boreal autumn SAM and winter precipitation over

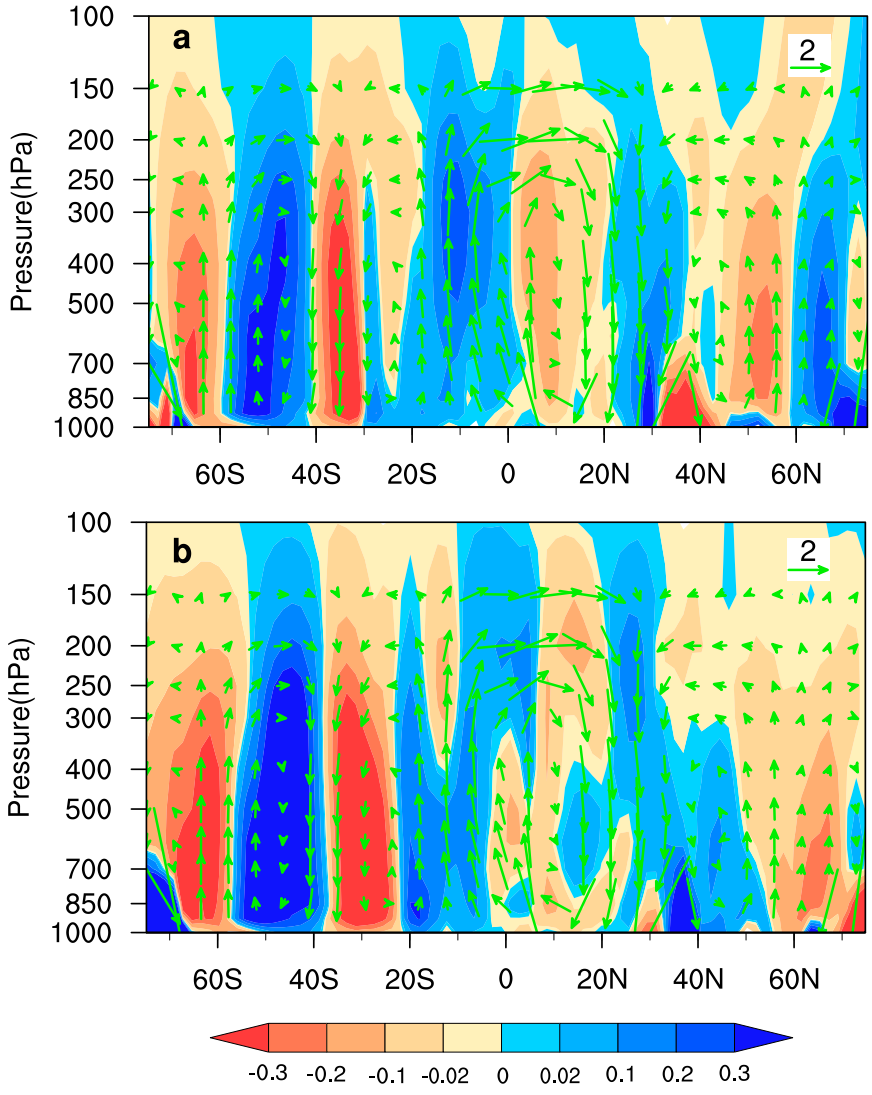

FIG. 8. Composite differences of the boreal winter vertical motion (10^{-4} Pa s^{-1}) in (a) EA and (b) EB response to the high and low boreal winter SOD-like SSTA forcing in the CAM5 model (shading). The vectors represent the climatological-mean boreal winter meridional circulation. The red (blue) shading corresponds to upward (downward) motion.

land in the NH. As an anomalous signal on a hemispheric scale, the SAM not only has an impact on regional climate anomalies but also affects the climate in the same latitude zone through the adjustment of the meridional circulation.

When the boreal autumn SAM is in its positive (negative) phase, anomalous divergence (convergence) at high levels and convergence (divergence) at low levels favor anomalous ascent (descent), which is superimposed on the climate mean states, strengthening (weakening) the upward branches near the equator and midlatitude regions in the NH. However, the situation is opposite over the subtropics (Figs. 3a,c). Suitable water vapor conditions (Fig. 3b) favor a positive (negative) tripole pattern in winter precipitation anomalies, with more (less) precipitation near the equator and midlatitude regions but less (more) precipitation over the subtropics (Figs. 1 and 2).

The difficulty in understanding the influence of the boreal autumn SAM on the NH winter precipitation lies in explaining how the anomalous preceding SAM signal persists and transmits to the NH in the next season. To resolve this issue, we investigated the roles of the SAM-related SST in the process. Evidence presented here suggests that a positive boreal autumn SAM event always induces strong westerlies with increases of ocean heat release south of 45°S and weak westerlies with decreases of ocean heat release over 30°–45°S (Fig. 4).

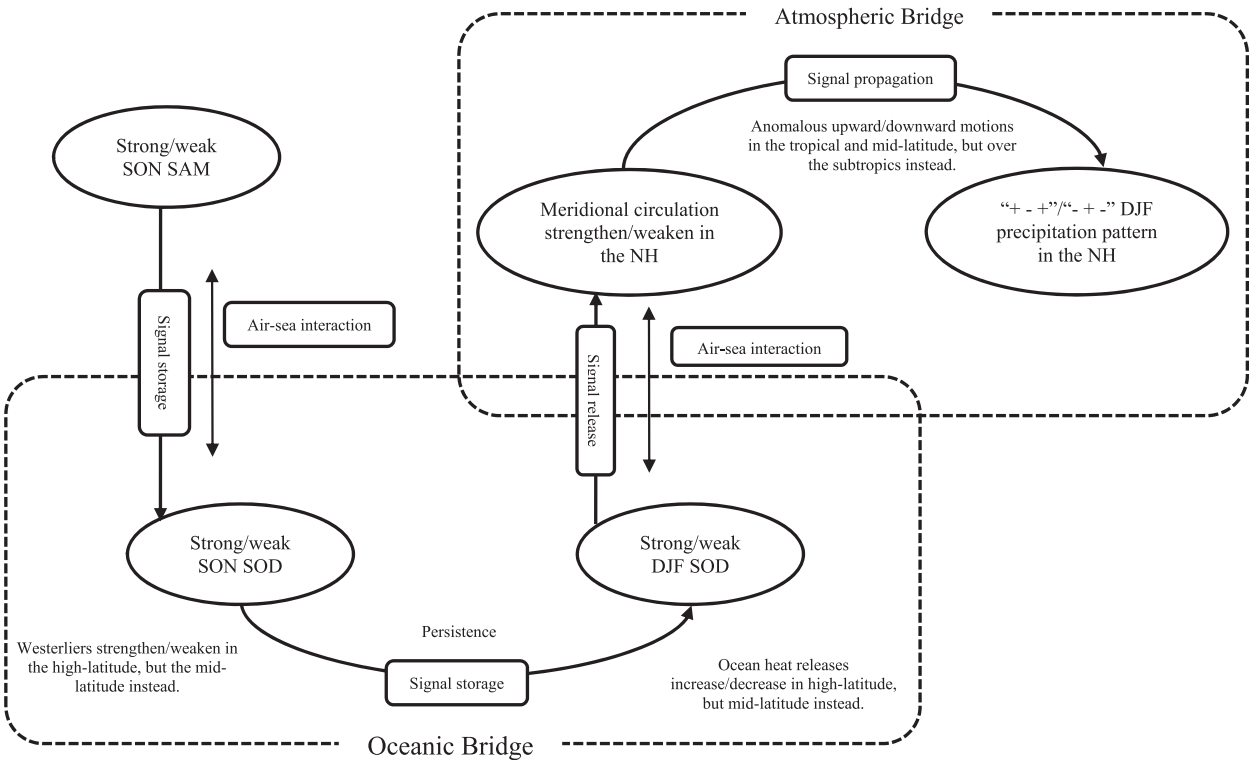

FIG. 9. Schematic representation of the effect of the boreal autumn SAM on winter precipitation over land in the NH.

At the same time, the anomalous westerlies result in equatorward Ekman transport of cold water, leading to negative SSTAs at SH high latitudes. The opposite situation occurs in midlatitudes. It is the combination of oceanic meridional heat advection and surface heat fluxes that imprints the strong autumn SAM signature onto the SST, with a warmer SST belt in midlatitudes and a colder belt in high latitudes in the SH. Such boreal autumn SOD anomalies can persist into the winter via the memory of SST (Fig. 5). When the boreal autumn SAM is weak, the situation is reversed.

The results of diagnostic analysis and numerical experiments both indicated that the SOD plays a bridging role in the effect of the boreal autumn SAM on winter precipitation in the NH (Figs. 6 and 8). A boreal autumn positive SAM event is usually associated with a positive SOD through autumn to winter. This SOD changes the meridional SST gradient and surface baroclinicity, which induce the anomalous eddy activities. The related convergence/divergence of the eddy heat flux balances the diabatic cooling/heating by adjustments of the vertical movement (Fig. 7). And meridional circulation exhibits corresponding adjustments to the positive SAM-related SOD, consisting of anomalous upward motion over 30°S and downward motion centered on 50°S. Given that the meridional circulation in the two hemispheres shares the same upward branch, changes in the SH meridional circulation lead to a simultaneous adjustment of the NH meridional circulation. Anomalous ascent and descent are superimposed on the climate mean state, which strengthens the upward motion centered on 10° and 50°N and downward motion at 30°N. In such a case, with a strong boreal autumn SAM, the NH winter precipitation anomalies tend to adopt a positive tripole pattern, with more precipitation over the equator and midlatitude regions but less precipitation in the subtropics. When the boreal autumn SAM is weak, this situation is reversed. The whole physical process represents an ocean–atmosphere coupled bridge (Li 2016), as shown in Fig. 9.

Our study suggests that the boreal autumn SAM may yield an additional predictor for the NH winter climate. Nevertheless, some scientific issues still remain. For instance, we note that there are zonally symmetric responses of NH winter precipitation to the boreal autumn SAM, but some differences still exist at the regional scale, especially in the levels of significance. Does the boreal autumn SAM simply provide some sort of background situation for winter precipitation in the NH? Do other regional climatic systems affect the regional precipitation anomalies based on this background? All of these issues are important to our understanding of the interaction between the hemispheres. This work highlights the influence of the boreal autumn SAM on the winter

precipitation in the NH. However, the problem remains of how to build a prediction model based on boreal autumn SAM and so improve the skill of the prediction of winter precipitation in the NH. This will require further research.

Acknowledgments. This work was jointly supported by the 973 Program (2013CB430200), the NSFC Key Project (41405086, 41030961), and the China Special Fund for Meteorological Research in the Public Interest (GYHY201306031). We appreciate the ECMWF for providing the reanalysis data. Precipitation data, ENSO index, and monthly mean ERSST data were provided by the NOAA/OAR/ESRL PSD. Comments and suggestions by three anonymous reviewers helped us to improve the paper.

REFERENCES

Adler, R. F., C. Kidd, G. Petty, M. Morrissey, and H. M. Goodman, 2001: Intercomparison of global precipitation products: The third Precipitation Intercomparison Project (PIP-3). *Bull. Amer. Meteor. Soc.*, **82**, 1377–1396, doi:10.1175/1520-0477(2001)082<1377:IOGPPT>2.3.CO;2.

——, G. Gu, J. J. Wang, G. J. Huffman, S. Curtis, and D. Bolvin, 2008: Relationships between global precipitation and surface temperature on interannual and longer timescales (1979–2006). *J. Geophys. Res.*, **113**, D22104, doi:10.1029/2008JD010536.

Boer, G., S. Fourest, and B. Yu, 2001: The signature of the annular modes in the moisture budget. *J. Climate*, **14**, 3655–3665, doi:10.1175/1520-0442(2001)014<3655:TSOTAM>2.0.CO;2.

Carleton, A. M., 2003: Atmospheric teleconnections involving the Southern Ocean. *J. Geophys. Res.*, **108**, 8080, doi:10.1029/2000JC000379.

Chen, G., R. A. Plumb, and J. Lu, 2010: Sensitivities of zonal mean atmospheric circulation to SST warming in an aqua-planet model. *Geophys. Res. Lett.*, **37**, L12701, doi:10.1029/2010GL043473.

Chen, M., P. Xie, J. E. Janowiak, and P. A. Arkin, 2002: Global land precipitation: A 50-yr monthly analysis based on gauge observations. *J. Hydrometeor.*, **3**, 249–266, doi:10.1175/1525-7541(2002)003<0249:GLPAYM>2.0.CO;2.

Ciasto, L. M., and D. W. Thompson, 2008: Observations of large-scale ocean–atmosphere interaction in the Southern Hemisphere. *J. Climate*, **21**, 1244–1259, doi:10.1175/2007JCLI1809.1.

——, M. A. Alexander, C. Deser, and M. H. England, 2011: On the persistence of cold-season SST anomalies associated with the annular modes. *J. Climate*, **24**, 2500–2515, doi:10.1175/2010JCLI3535.1.

Dee, D. P., and Coauthors, 2011: The ERA-Interim reanalysis: Configuration and performance of the data assimilation system. *Quart. J. Roy. Meteor. Soc.*, **137**, 553–597, doi:10.1002/qj.828.

Ding, Q., E. J. Steig, D. S. Battisti, and J. M. Wallace, 2012: Influence of the tropics on the southern annular mode. *J. Climate*, **25**, 6330–6348, doi:10.1175/JCLI-D-11-00523.1.

Ding, R., J. P. Li, and Y.-H. Tseng, 2015: The impact of South Pacific extratropical forcing on ENSO and comparisons with the North Pacific. *Climate Dyn.*, **44**, 2017–2034, doi:10.1007/s00382-014-2303-5.

Fan, K., and H. Wang, 2004: Antarctic Oscillation and the dust weather frequency in north China. *Geophys. Res. Lett.*, **31**, L10201, doi:10.1029/2004GL019465.

Feng, J., J. P. Li, and Y. Li, 2010: Is there a relationship between the SAM and southwest Western Australian winter rainfall? *J. Climate*, **23**, 6082–6089, doi:10.1175/2010JCLI3667.1.

Fogt, R. L., and D. H. Bromwich, 2006: Decadal variability of the ENSO teleconnection to the high-latitude South Pacific governed by coupling with the southern annular mode. *J. Climate*, **19**, 979–997, doi:10.1175/JCLI3671.1.

——, J. M. Jones, and J. Renwick, 2012: Seasonal zonal asymmetries in the southern annular mode and their impact on regional temperature anomalies. *J. Climate*, **25**, 6253–6270, doi:10.1175/JCLI-D-11-00474.1.

Frierson, D. M., J. Lu, and G. Chen, 2007: Width of the Hadley cell in simple and comprehensive general circulation models. *Geophys. Res. Lett.*, **34**, L18804, doi:10.1029/2007GL031115.

Gillett, N., T. Kell, and P. Jones, 2006: Regional climate impacts of the southern annular mode. *Geophys. Res. Lett.*, **33**, L23704, doi:10.1029/2006GL027721.

Gong, D., and S. Wang, 1998: Antarctic Oscillation: Concept and applications. *Chin. Sci. Bull.*, **43**, 734–738, doi:10.1007/BF02898949.

——, and ——, 1999: Definition of Antarctic Oscillation index. *Geophys. Res. Lett.*, **26**, 459–462, doi:10.1029/1999GL900003.

Hall, A., and M. Visbeck, 2002: Synchronous variability in the Southern Hemisphere atmosphere, sea ice, and ocean resulting from the annular mode. *J. Climate*, **15**, 3043–3057, doi:10.1175/1520-0442(2002)015<3043:SVITSH>2.0.CO;2.

Hartmann, D. L., and F. Lo, 1998: Wave-driven zonal flow vacillation in the Southern Hemisphere. *J. Atmos. Sci.*, **55**, 1303–1315, doi:10.1175/1520-0469(1998)055<1303:WDZFVI>2.0.CO;2.

Hendon, H. H., D. W. Thompson, and M. C. Wheeler, 2007: Australian rainfall and surface temperature variations associated with the Southern Hemisphere annular mode. *J. Climate*, **20**, 2452–2467, doi:10.1175/JCLI4134.1.

Holton, J. R., and G. J. Hakim, 2012: *An Introduction to Dynamic Meteorology*. 5th ed. Elsevier Academic Press, 552 pp.

Hoskins, B. J., and D. J. Karoly, 1981: The steady linear response of a spherical atmosphere to thermal and orographic forcing. *J. Atmos. Sci.*, **38**, 1179–1196, doi:10.1175/1520-0469(1981)038<1179:TSLROA>2.0.CO;2.

Huffman, G. J., and D. T. Bolvin, 2011: GPCP version 2.2 combined precipitation data set documentation. [Available online at ftp://precip.gsfc.nasa.gov/pub/gpcp-v2.2/doc/V2.2_doc.pdf.]

Kalnay, E., and Coauthors, 1996: The NCEP/NCAR 40-Year Reanalysis Project. *Bull. Amer. Meteor. Soc.*, **77**, 437–471, doi:10.1175/1520-0477(1996)077<0437:TNYRP>2.0.CO;2.

Kidston, J., J. Renwick, and J. McGregor, 2009: Hemispheric-scale seasonality of the southern annular mode and impacts on the climate of New Zealand. *J. Climate*, **22**, 4759–4770, doi:10.1175/2009JCLI2640.1.

Lefebvre, W., H. Goosse, R. Timmermann, and T. Fichefet, 2004: Influence of the southern annular mode on the sea ice–ocean system. *J. Geophys. Res.*, **109**, C09005, doi:10.1029/2004JC002403.

L'Heureux, M. L., and D. W. J. Thompson, 2006: Observed relationships between the El Niño–Southern Oscillation and the extratropical zonal-mean circulation. *J. Climate*, **19**, 276–287, doi:10.1175/JCLI3617.1.

Li, J. P., 2005: Physical nature of the Arctic Oscillation and its relationship with East Asian atmospheric circulation (in Chinese). *Air–Sea–Land Interaction in Asia Monsoon Region and Their Impacts on the Climate Variation in China*, Q. Yu et al., Eds., China Meteorological Press, 169–176.

——, and J. X. Wang, 2003: A modified zonal index and its physical sense. *Geophys. Res. Lett.*, **30**, 1632, doi:10.1029/2003GL017441.

——, and Coauthors, 2013: Progress in air–land–sea interactions in Asia and their role in global and Asian climate change (in Chinese). *Chin. J. Atmos. Sci.*, **37**, 518–538.

——, 2016: Impacts of annular modes on extreme climate events over the East Asian monsoon region. *Dynamics and Predictability of Large-Scale, High-Impact Weather and Climate Events*, J. P. Li et al., Eds., Cambridge University Press, in press.

Li, Y., J. P. Li, and J. Feng, 2012: A teleconnection between the reduction of rainfall in southwest Western Australia and north China. *J. Climate*, **25**, 8444–8461, doi:10.1175/JCLI-D-11-00613.1.

Limpasuvan, V., and D. L. Hartmann, 1999: Eddies and the annular modes of climate variability. *Geophys. Res. Lett.*, **26**, 3133–3136, doi:10.1029/1999GL010478.

——, and ——, 2000: Wave-maintained annular modes of climate variability. *J. Climate*, **13**, 4414–4429, doi:10.1175/1520-0442(2000)013<4414:WMAMOC>2.0.CO;2.

Liu, J., X. Yuan, D. Rind, and D. G. Martinson, 2002: Mechanism study of the ENSO and southern high latitude climate teleconnections. *Geophys. Res. Lett.*, **29**, 1679, doi:10.1029/2002GL015143.

——, J. A. Curry, and D. G. Martinson, 2004: Interpretation of recent Antarctic sea ice variability. *Geophys. Res. Lett.*, **31**, L02205, doi:10.1029/2003GL018732.

Lorenz, D. J., and D. L. Hartmann, 2001: Eddy–zonal flow feedback in the Southern Hemisphere. *J. Atmos. Sci.*, **58**, 3312–3327, doi:10.1175/1520-0469(2001)058<3312:EZFFIT>2.0.CO;2.

Marshall, G. J., and W. M. Connolley, 2006: Effect of changing Southern Hemisphere winter sea surface temperatures on southern annular mode strength. *Geophys. Res. Lett.*, **33**, L17717, doi:10.1029/2006GL026627.

——, A. Orr, N. P. van Lipzig, and J. C. King, 2006: The impact of a changing Southern Hemisphere annular mode on Antarctic Peninsula summer temperatures. *J. Climate*, **19**, 5388–5404, doi:10.1175/JCLI3844.1.

Nan, S., and J. Li, 2003: The relationship between the summer precipitation in the Yangtze River valley and the boreal spring Southern Hemisphere annular mode. *Geophys. Res. Lett.*, **30**, 2266, doi:10.1029/2003GL018381.

——, and ——, 2005a: The relationship between the summer precipitation in the Yangtze River valley and the boreal spring Southern Hemisphere annular mode: I. Basic facts (in Chinese). *Acta Meteor. Sin.*, **63**, 837–846.

——, and ——, 2005b: The relationship between the summer precipitation in the Yangtze River valley and the boreal spring Southern Hemisphere annular mode: II. The role of the Indian Ocean and South China Sea as an ''oceanic bridge'' (in Chinese). *Acta Meteor. Sin.*, **63**, 847–856.

Pyper, B. J., and R. M. Peterman, 1998: Comparison of methods to account for autocorrelation in correlation analyses of fish data. *Can. J. Fish. Aquat. Sci.*, **55**, 2127–2140, doi:10.1139/f98-104.

Reason, C., and M. Rouault, 2005: Links between the Antarctic Oscillation and winter rainfall over western South Africa. *Geophys. Res. Lett.*, **32**, L07705, doi:10.1029/2005GL022419.

Renwick, J., and D. Thompson, 2006: The southern annular mode and New Zealand climate. *Water Atmos.*, **14**, 24–25.

Rudolf, B., and U. Schneider, 2005: Calculation of gridded precipitation data for the global land-surface using in-situ gauge observations. *Proc. Second Workshop of the Int. Precipitation Working Group*, Offenbach, Germany, WMO, 231–247.

Sen Gupta, A., and M. H. England, 2006: Coupled ocean–atmosphere–ice response to variations in the southern annular mode. *J. Climate*, **19**, 4457–4486, doi:10.1175/JCLI3843.1.

Silvestri, G. E., and C. S. Vera, 2003: Antarctic Oscillation signal on precipitation anomalies over southeastern South America. *Geophys. Res. Lett.*, **30**, 2115, doi:10.1029/2003GL018277.

Smith, T. M., R. W. Reynolds, T. C. Peterson, and J. Lawrimore, 2008: Improvements to NOAA's historical merged land-ocean surface temperature analysis (1880–2006). *J. Climate*, **21**, 2283–2296, doi:10.1175/2007JCLI2100.1.

Sun, J., 2010: Possible impact of the boreal spring Antarctic Oscillation on the North American summer monsoon. *Atmos. Oceanic Sci. Lett.*, **3**, 232–236, doi:10.1080/16742834.2010.11446870.

——, H. Wang, and W. Yuan, 2010: Linkage of the boreal spring Antarctic Oscillation to the West African summer monsoon. *J. Meteor. Soc. Japan*, **88**, 15–28, doi:10.2151/jmsj.2010-102.

Thompson, D. W., and J. M. Wallace, 2000: Annular modes in the extratropical circulation. Part I: Month-to-month variability. *J. Climate*, **13**, 1000–1016, doi:10.1175/1520-0442(2000)013<1000:AMITEC>2.0.CO;2.

——, and S. Solomon, 2002: Interpretation of recent Southern Hemisphere climate change. *Science*, **296**, 895–899, doi:10.1126/science.1069270.

Ummenhofer, C. C., and M. H. England, 2007: Interannual extremes in New Zealand precipitation linked to modes of Southern Hemisphere climate variability. *J. Climate*, **20**, 5418–5440, doi:10.1175/2007JCLI1430.1.

——, A. Sen Gupta, and M. H. England, 2009: Causes of late twentieth-century trends in New Zealand precipitation. *J. Climate*, **22**, 3–19, doi:10.1175/2008JCLI2323.1.

Wu, Z. W., J. H. He, J. P. Li, and Z. H. Jiang, 2006a: The summer drought-flood coexistence in the middle and lower reaches of the Yangtze River and analysis of its air-sea background feathers in anomalous years (in Chinese). *Chin. J. Atmos. Sci.*, **30**, 570–577.

——, J. P. Li, J. H. He, and Z. H. Jiang, 2006b: Large-scale atmospheric singularities and summer long-cycle droughts-floods abrupt alternation in the middle and lower reaches of the Yangtze River. *Chin. Sci. Bull.*, **51**, 2027–2034, doi:10.1007/s11434-006-2060-x.

——, ——, B. Wang, and X. Liu, 2009: Can the Southern Hemisphere annular mode affect China winter monsoon? *J. Geophys. Res.*, **114**, D11107, doi:10.1029/2008JD011501.

——, J. Dou, and H. Lin, 2015: Potential influence of the November–December Southern Hemisphere annular mode on the East Asian winter precipitation: A new mechanism. *Climate Dyn.*, **44**, 1215–1226, doi:10.1007/s00382-014-2241-2.

Xie, P., and P. A. Arkin, 1997: Global precipitation: A 17-year monthly analysis based on gauge observations, satellite estimates and numerical model outputs. *Bull. Amer. Meteor. Soc.*, **78**, 2539–2558, doi:10.1175/1520-0477(1997)078<2539:GPAYMA>2.0.CO;2.

Yuan, X., and C. Li, 2008: Climate modes in southern high latitudes and their impacts on Antarctic sea ice. *J. Geophys. Res.*, **113**, C06S91, doi:10.1029/2006JC004067.

Zheng, F., and J. P. Li, 2012: Impact of preceding boreal winter Southern Hemisphere annular mode on spring precipitation over south China and related mechanism (in Chinese). *Chin. J. Geophys.*, **55**, 3542–3557.

——, ——, and T. Liu, 2014: Some advances in studies of the climatic impacts of the Southern Hemisphere annular mode. *J. Meteor. Res.*, **28**, 820–835, doi:10.1007/s13351-014-4079-2.

——, ——, L. Wang, F. Xie, and X. Li, 2015: Cross-seasonal influence of the December–February Southern Hemisphere annular mode on March–May meridional circulation and precipitation. *J. Climate*, **28**, 6859–6881, doi:10.1175/JCLI-D-14-00515.1.